

## Structure of the high-pressure phase III of iron sulfide

R. J. Nelmes

*Department of Physics and Astronomy, The University of Edinburgh, Edinburgh EH9 3JZ, United Kingdom*

M. I. McMahon\*

*Department of Physics, The University of Liverpool, Liverpool L69 7ZE, United Kingdom*

S. A. Belmonte

*Department of Physics and Astronomy, The University of Edinburgh, Edinburgh EH9 3JZ, United Kingdom*

J. B. Parise

*Center for High Pressure Research and Department of Earth and Space Sciences, State University of New York, Stony Brook, New York 11794-2100*

(Received 29 April 1998)

The structure of FeS-III has been solved from angle-dispersive x-ray powder-diffraction data collected at 7.5 GPa and room temperature. It has a monoclinic unit cell (space group  $P2_1/a$ ) containing 12 formula units. The loss of the magnetic order at the transition from phase II is accompanied by a sharp reduction in Fe-Fe distances to  $\sim 2.7$  Å. These short contacts form a  $3d$  network of four-atom clusters and six-, eight-, and ten-member rings. [S0163-1829(99)01713-0]

Iron sulfide has long attracted attention as a simple transition-metal compound with a range of interesting electronic properties. It is an antiferromagnetic semiconductor in the troilite phase at ambient pressure and temperature; it has a spin-flip transition on heating, then becoming paramagnetic above a Néel temperature of  $\sim 600$  K; and it passes through a semiconductor-to-metal transition under pressure.<sup>1,2</sup> The troilite structure is unique to FeS, and contains triangular clusters of Fe atoms that—with the magnetism—signal a mixed localized/itinerant character in the  $3d$  electrons.<sup>3</sup> The properties of the iron-sulfur system, and of FeS in particular, are also of major interest and importance in geoplanetary science. Sulfur is one of the candidates to account for the evidence that the density of the Earth's outer core is significantly lower than that of pure iron.<sup>4</sup> The solid core of Mars is believed to be composed of Fe, or an Fe-Ni alloy, and some 14% of S by weight.<sup>5,6</sup> Other terrestrial planets and satellites are also expected to have similar sulfur-containing ferrous cores.

Lively interest in FeS at high pressure was sparked by the proposal—some 30 years ago—that sulfur may be a major component of the Earth's core<sup>4</sup> and by the discovery, at about the same time, of troilite in lunar samples.<sup>7</sup> A number of high-pressure studies in the 1970's revealed transitions from the semiconducting troilite phase to a more metallic FeS-II phase at 3.4 GPa, and then to another phase FeS-III at 6.7 GPa,<sup>8</sup> which remains stable to at least 60 GPa at room temperature.<sup>9</sup> Despite various attempts, no clear structure determinations were obtained until King and Prewitt showed FeS-II to have the MnP structure.<sup>8</sup> They were unable to solve the structure of FeS-III, but estimated a significant density increase of  $\sim 9\%$  at the MnP/FeS-III transition. Mössbauer studies indicate that this is a semimetal to metal transition, at which the magnetic ordering of the troilite and MnP phases is lost.<sup>2,10</sup> Fei *et al.* recently carried out diffraction studies of FeS under high pressure at high temperature, and proposed a

high  $P$ - $T$  phase IV whose density leads to a re-estimate of the size of the Martian core.<sup>11</sup> There appears to be an abrupt density increase in this phase at a pressure close to that of the MnP/FeS-III transition, and hence phase IV is likely to exhibit similar structural changes, and to be paramagnetic and metallic at high pressures.<sup>11</sup>

The structure of phase III is thus a key to understanding the electronic properties and the high-pressure behavior of FeS, and repeated attempts have been made to solve what appears to be a quite complex structure. Most recently, Fei *et al.* reported a possible monoclinic unit cell,<sup>11</sup> and Kusaba *et al.* obtained a good fit to all peak positions in the powder pattern with a larger monoclinic cell containing 12 formula units.<sup>12</sup> But no further progress was made in determining the crystal structure. We have now solved the full structure from angle-dispersive powder-diffraction data collected at room temperature.<sup>13</sup> The Fe-S coordination is quite strongly distorted, and the short Fe-Fe distances appear to form an intriguing network of clusters, and six-, eight-, and ten-atom rings.

The sample material was prepared by heating a stoichiometric mixture of iron—which had previously been reduced at 1100 K in a stream of hydrogen gas for 1 h—and sulfur at 923 K for 10 days in an evacuated silica glass capsule. Diffraction data were collected at room temperature on station 9.1 at the Synchrotron Radiation Source, Daresbury Laboratory, using an image-plate area detector.<sup>14</sup> The incident wavelength was 0.4654(1) Å. Finely ground troilite was loaded into diamond-anvil cells with 4:1 methanol:ethanol as a pressure transmitting medium and chips of ruby for pressure measurement.

Powder patterns collected in the troilite and MnP phases gave excellent fits to the known structures, as shown in Fig. 1 for the MnP phase. The refined lattice parameters for troilite at ambient pressure are  $a = 5.9655(3)$  Å and  $c = 11.7512(3)$  Å, in agreement with the values for stoichio-

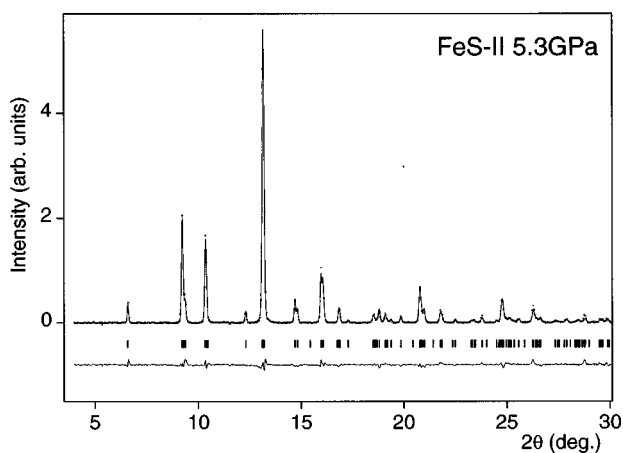


FIG. 1. Rietveld refinement fit (line) to an integrated profile (points) for the MnP phase of FeS at 5.3 GPa (at room temperature). Tick marks show the positions of all reflections allowed by symmetry. The difference between the observed and calculated profiles is shown below the tick marks.

metric FeS,<sup>8</sup> and the patterns contained no evidence of any other phase above the detection limit of  $\sim 0.5\%$ . The refined atomic coordinates of both phases are in good agreement (within 0.002) with the single-crystal results.<sup>8</sup> The troilite and MnP phases of FeS both have structures based on the NiAs structure,<sup>8</sup> to which they both transform on heating above  $\sim 600$  K.<sup>11</sup> The NiAs cell, with hexagonal lattice parameters  $A=B$  and  $C$ , contains two formula units. Figure 2 illustrates how the NiAs cell is related to those of the troilite and MnP phases. Troilite has a superstructure of NiAs, which has a six-times larger hexagonal ( $P\bar{6}2c$ ) cell with lattice parameters related to the NiAs cell by  $a''=A-B$  ( $\sqrt{3}A$  in magnitude) and  $c''=2C$ . The MnP phase has a different superstructure, with an orthorhombic ( $Pnma$ ) cell containing four formula units, in which the lattice parameters are related by  $a'=C$ ,  $b'=A$  and  $c'=\sim A+2B$  ( $\sqrt{3}A$  in magnitude).<sup>8</sup> In the NiAs structure, the S and Fe layers alternate along the  $C$  axis, such that the S atoms are coordinated by six Fe atoms arranged in a trigonal prism, and the Fe atoms are coordinated by six S atoms arranged in an octahedron.<sup>8</sup>

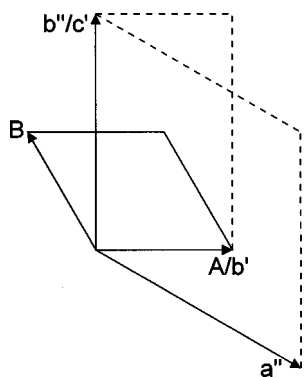


FIG. 2. Relationship of the NiAs ( $A$  and  $B$ ), troilite ( $a''$  and  $b''$ ), and MnP ( $b'$  and  $c'$ ) unit cells. The lattice parameters perpendicular to the plane of the drawing are, respectively,  $C$ ,  $c''=2c$  and  $a'=C$ .

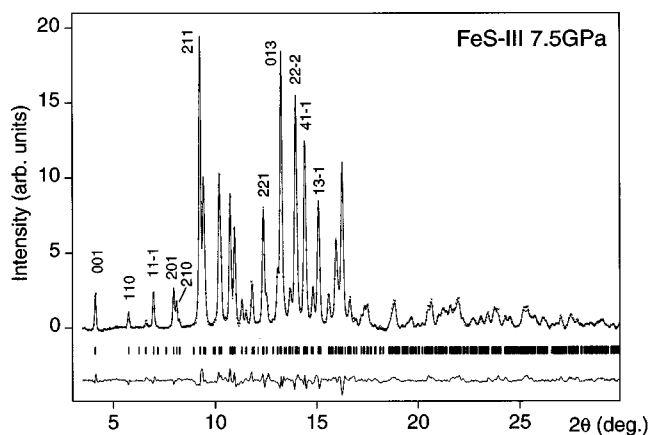


FIG. 3. Rietveld refinement fit (line) to an integrated profile (points) from FeS-III at 7.5 GPa (at room temperature). Tick marks show the positions of all reflections allowed by symmetry. The difference between the observed and calculated profiles is shown below the tick marks. Indexed reflections include the strongest from the NiAs subcell ( $h+k+l=2n$ ,  $h+l=3n$ ), some of the superlattice reflections in common with the MnP phase ( $h+k+l=2n$ ), and some of the additional superlattice reflections of the FeS-III phase ( $h+l\neq 3n$ ). 11-1 denotes the  $(11\bar{1})$  reflection, etc.

Figure 3 shows a powder pattern obtained in phase III at 7.5 GPa; it is very similar in its general features to the energy-dispersive patterns of Kusaba *et al.*,<sup>12</sup> though there are some significant differences in relative peak intensities. Attempts to index this pattern using the program DICVOL (Ref. 15) yielded as the best-fitting solution a monoclinic cell with  $a=8.11$  Å,  $b=5.66$  Å,  $c=6.48$  Å, and  $\beta=93.0^\circ$ —the same as the cell found independently by Kusaba *et al.*<sup>12</sup> Considerations of symmetry and density indicate, as said, that this cell contains 12 formula units. When indexed on this cell,  $(h0l)$  reflections with  $h$ =odd and  $(0k0)$  reflections with  $k$ =odd are systematically absent, consistent with space group  $P2_1/a$ .<sup>16</sup>

The study by King and Prewitt<sup>8</sup> showed that a single crystal of troilite passes through the transitions to MnP and FeS-III without losing its integrity, apart from twinning. This strongly suggests that the general framework of the structure is preserved, with the transitions proceeding by relatively small displacements rather than reconstruction. Their results also revealed a strong contraction of the unit cell along the NiAs  $C$ -axis direction, by some 9%, on passing from the MnP to FeS-III phase. Furthermore, they reported the appearance of “cell-doubling” reflections in the hexagonal basal plane, i.e., the  $0kl$  layer of the MnP phase. In the MnP phase, the only reflections in this layer are those corresponding to the NiAs unit cell; the additional, superlattice reflections of MnP—i.e.,  $(001)$ ,  $(003)$ ,  $(010)$ ,  $(012)$ , etc.—are all systematically absent for space group  $Pnma$ . New reflections at these positions—halfway between the NiAs reflections—indicate that the  $n$ -glide symmetry is lost in FeS-III.

The only setting of the FeS-III cell consistent with all of this has the unique monoclinic  $b$  axis along the  $c'$  axis of MnP, and the  $a$  and  $c$  axes in the  $a'b'$  plane of MnP, such that  $a=a'+2b'$ ,  $b=-c'$ , and  $c=b'-a'$ . This relationship is shown in Fig. 4, which also includes the MnP-type unit cell corresponding to the FeS-III cell—having  $a'=1/3(a-2c)=5.218$  Å in magnitude.  $b'=1/3(a+c)=3.370$  Å,  $c'$

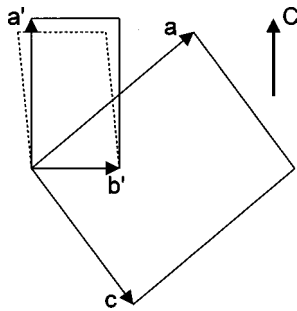


FIG. 4. Relationship of the  $ac$  plane of the FeS-III unit cell to the  $a'b'$  plane of the MnP unit cell. The dashed line shows how the MnP cell distorts in the FeS-III structure. The direction of the NiAs  $C$  axis is marked.

$= -b = 5.667 \text{ \AA}$ , and  $\gamma = 95.62^\circ$ . (We note that the latter is the cell proposed by Fei *et al.*,<sup>11</sup> with their  $b$  and  $c$  axes interchanged.) It can be seen in Fig. 4 that the effects of the transition are (i) the large contraction of  $a'$  (along the NiAs  $C$  axis) previously reported,<sup>8</sup> and (ii) a pronounced monoclinic shearing of the MnP  $a'b'$  plane, which lies perpendicular to the NiAs basal plane.<sup>17</sup>

The FeS-III unit cell retains the lattice repeat of the MnP structure along  $b$  ( $c'$  of MnP), but has three times the area of the MnP cell in the  $ac$  plane ( $a'b'$  of MnP). The relative orientation of the FeS-III cell indicates that the  $a$ -glide symmetry and a third of the  $2_1$  axes of  $Pnma$  are retained.<sup>18</sup> If the NiAs structure is described in the FeS-III cell, the Fe atoms are in three independent four-fold sites with Fe(1) at  $(1/12, 3/4, 1/12)$ , Fe(2) at  $(1/4, 1/4, 1/4)$ , and Fe(3) at  $(5/12, 3/4, 5/12)$ , and likewise for the S atoms with S(1) at  $(1/6, 1/12, 11/12)$ , S(2) at  $(1/2, 11/12, 3/4)$ , and S(3) at  $(1/3, 5/12, 7/12)$ . The profile in Fig. 3 contains NiAs reflections, the additional superlattice reflections of the MnP phase (with  $h+k+l \neq 2n$ ), and the further new reflections of FeS-III (with  $h+l \neq 3n$ ). Among the latter is the lowest-angle line which indexes as (001). This reflection indicates that some atoms that are  $c/2$  apart in NiAs (and MnP) are displaced in  $z$  to a separation  $\neq c/2$ —probably Fe atoms in view of the strength of (001). The Fe(1) and Fe(3) groups of atoms are  $c/2$  apart, but the symmetry does not allow this to alter significantly. However, the Fe(2) atoms are in two pairs  $c/2$  apart in the NiAs structure, and their separation is a variable in the FeS-III symmetry. Furthermore, the retention of the MnP superlattice reflections and the same lattice repeat along  $b$  suggests that the  $y$  coordinates of FeS-III are similar to those of the MnP phase. A trial structure was thus adopted with the  $y$  coordinates of MnP and the  $x$  and  $z$  coordinates of NiAs (as above), except that Fe(2) was displaced  $\sim 0.01$  along  $z$ . From this starting model, rapid convergence was obtained to the fit shown in Fig. 3, using the Rietveld refinement program GSAS.<sup>19</sup> This fit includes a parameter to describe a small degree of preferred orientation—the form and magnitude of which was checked independently by recording a pattern with the axis of the pressure cell inclined to the incident beam.<sup>21</sup> Test refinements in the lower-symmetry spacegroups  $P2_1$  and  $Pa$  gave no significant further improvements in fit.

The refined lattice parameters and atomic coordinates are given in Table I. This is a complex structure to determine from high-pressure powder-diffraction data. To estimate the

TABLE I. Atomic coordinates of FeS-III in the  $4(e)$  sites of  $P2_1/a$  at 7.5 GPa, (i) as obtained ( $\times 10^4$ ) from the data in Fig. 3, and (ii) as the average ( $\times 10^3$ ) of values from three different samples, with refined lattice parameters  $a = 8.1103(3) \text{ \AA}$ ,  $b = 5.6666(2) \text{ \AA}$ ,  $c = 6.4832(2) \text{ \AA}$ , and  $\beta = 93.050(3)^\circ$ .

	(i) Best fit			(ii) Average		
	$x$	$y$	$z$	$x$	$y$	$z$
Fe(1)	655(5)	7988(6)	829(5)	65(2)	800(4)	82(2)
Fe(2)	2120(4)	2139(8)	1803(5)	211(2)	212(3)	178(3)
Fe(3)	4220(6)	7607(6)	4489(6)	423(1)	763(2)	450(2)
S(1)	1845(8)	779(14)	8652(7)	188(4)	76(4)	865(3)
S(2)	5182(9)	9110(10)	7547(7)	519(3)	911(2)	756(6)
S(3)	3321(9)	4163(11)	5922(8)	335(3)	420(3)	591(1)

true accuracy of the refined coordinates, patterns were collected and refined in the same way from two other samples, in one of which there was no detectable preferred orientation.<sup>21</sup> The average values from the three samples are given under (ii) in Table I, and we will use these values in describing and discussing the structure.

Figure 5 shows the array of Fe atoms in FeS-III, viewed approximately along the  $b$  axis. The solid lines join atoms less than  $3.0 \text{ \AA}$  apart, which is a reasonable criterion for Fe-Fe bonding brought about by delocalization of  $3d$  electrons.<sup>3</sup> The direction corresponding to the NiAs  $C$  axis is

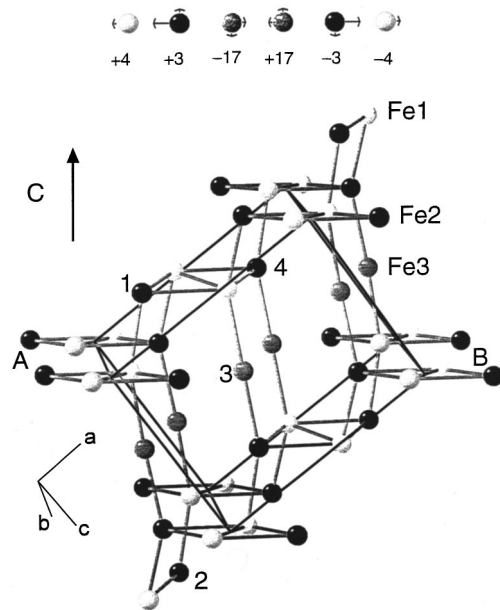


FIG. 5. Arrangement of the Fe atoms in FeS-III at 7.5 GPa. Fe(1), Fe(2), and Fe(3) atoms are shown as white, black, and grey spheres, respectively. Links between atoms mark all Fe-Fe distances  $< 3.0 \text{ \AA}$ . Unit cell axes  $a$ ,  $b$ , and  $c$  are shown.  $AB$  marks the basal plane of the NiAs substructure, and the arrow marks the direction of its  $C$  axis. Displacements from MnP positions are shown at the top of the figure for the atoms within the marked cell in the  $AB$  plane—as arrows of length proportional to the displacements in  $AB$  and along  $C$  (the largest, for Fe(2) along  $AB$ , is  $0.52 \text{ \AA}$ ), and as “+4,” “+3,” etc. in units of  $0.01 \text{ \AA}$  along  $\pm b$ . Atoms labeled 1 and 2 are in a ten-member ring, 1 and 3 are in an eight-member ring, and 3 and 4 are in a six-member ring.

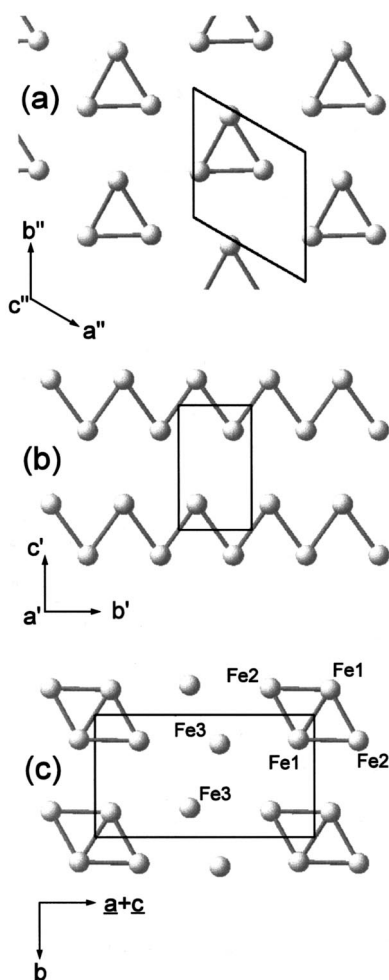


FIG. 6. Comparison of the Fe-atom arrays in the basal plane, perpendicular to  $C$ , for the (a) troilite, (b) MnP, and (c) FeS-III phases of FeS. All are drawn on a common scale, and in the relative orientations shown in Figs. 2 and 4. The unit cell in the basal plane is outlined. Fe(1), Fe(2), and Fe(3) atoms are distinguished in (c).

marked (parallel to  $c''$  of the troilite phase and  $a'$  of the MnP phase). The Fe atoms can thus be seen to lie close to planes, stacked along  $C$ , parallel to the basal planes of the NiAs structure—as they do in the troilite and MnP structures. The Fe(1), Fe(2), and Fe(3) atoms are shown, respectively, as white, black, and grey spheres. At the top of the figure, the displacements relative to the MnP phase coordinates are shown for the Fe(1), Fe(2), Fe(3), Fe(3), Fe(2), and Fe(1) atoms lying in the central basal plane (labeled  $AB$ ) within the marked unit cell. As the displacements indicate, there is a center of inversion symmetry at the midpoint of this group.

Figure 6 compares the Fe-atom arrays in the basal plane, perpendicular to  $C$ , for the troilite, MnP and FeS-III phases. As in Fig. 5, solid lines join atoms less than 3.0 Å apart. In the troilite phase, the Fe atoms are clustered into triangles in the basal planes, with Fe-Fe distances of  $\leq 2.9$  Å, and in the MnP phase, the Fe atoms displace differently to form zigzag chains running along  $b'$ , again with Fe-Fe distances  $\leq 2.9$  Å. In both phases, the basal-plane units (the triangles and chains) are linked by Fe-Fe distances of  $\leq 2.9$  Å along  $C$ . The structural characteristic of clustering in the basal plane, with the clusters linked along  $C$ , is retained in phase III, but in a more complex way. As shown in Figs. 5 and 6(c), the

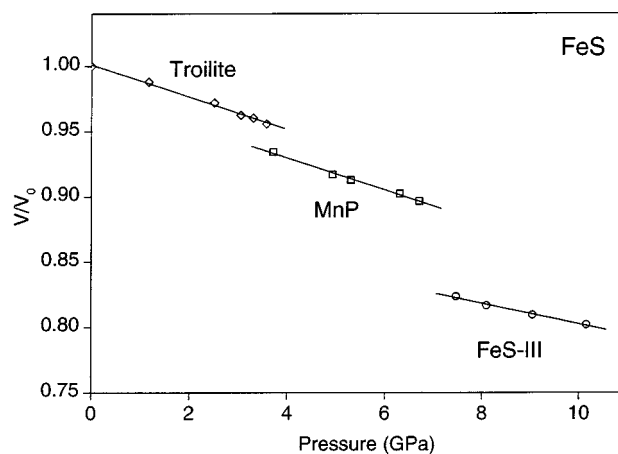


FIG. 7.  $V/V_0$  as a function of pressure through the troilite, MnP and FeS-III phases of FeS. The lines are guides to the eye only.

Fe(1) and Fe(2) atoms move such as to separate from the Fe(3) atoms [the shortest basal-plane Fe(2)-Fe(3) distance is 3.50(2) Å], and thereby break the  $b'$  axis chains of the MnP phase and form clusters in which four atoms lie in a close-packed arrangement. The five short Fe-Fe distances in these clusters are all in the range  $2.70 \pm 0.03$  Å. In Fig. 6 and at the top of Fig. 5, the Fe(3) atoms can be seen also to move apart along  $b$  (by  $\pm 0.17$  Å), which reduces the interaction they had in the zigzag chains of the MnP phase; the minimum Fe(3)-Fe(3) distance is now 3.02(2) Å. Despite this large rearrangement, the overall dimensions of the basal planes change little from the MnP phase, as can be seen by comparing Fig. 6(b) and 6(c): refinement of a mixed-phase pattern at 7.1 GPa shows<sup>20</sup> that the FeS-III lattice repeat along  $AB$  is 1.5% greater than  $3b'$ , while  $b$  is 0.6% less than  $c'$ . However, as shown in Fig. 4, the stacking of planes along  $C$  is sheared  $\rightleftharpoons$  by  $6^\circ$  and their separation is reduced by 7.6%, and these changes lead to marked reductions in the Fe-Fe distances along  $C$  also. The four-atom clusters are linked into staggered  $ab$  sheets by Fe(2)-Fe(1) bonds (Fig. 5) that are additionally reduced by the Fe(2) displacement along  $C$  to only 2.59(2) Å. And these sheets are crosslinked along  $c$  by Fe(2)-Fe(3)-Fe(1) bonds in which both Fe-Fe distances are 2.72(2) Å—the same within error as in the four-atom clusters. All other Fe-Fe distances are  $> 3.0$  Å. Those less than 3.0 Å form the complex three-dimensional framework shown in Fig. 5, comprising six-, eight-, and ten-atom rings, crosslinked by the four-atom clusters.

Fe(1) and Fe(3) have S-atom coordination similar to the troilite phase, forming quite distorted FeS<sub>6</sub> octahedra; the Fe-S bond lengths around Fe(1) range from 2.21(4) to 2.55(3) Å, and those around Fe(3) range from 2.25(4) to 2.43(2) Å, compared with 2.36 to 2.72 Å in troilite at ambient pressure.<sup>8</sup> However, Fe(2) is reduced to fivefold close coordination, in an approximately regular square pyramid of S atoms with Fe-S distances ranging from 2.17(3) to 2.32(3) Å. The large displacement of Fe(2) increases the sixth distance—to one of the S(3) atoms—to 3.05(2) Å.

Figure 7 shows how the volume per formula unit decreases through the troilite, MnP, and FeS-III phases up to 10 GPa, and Table II gives the refined lattice parameters at the lowest and highest pressure points shown for each phase in Fig. 7. The data shown in Fig. 7 are not of sufficient

TABLE II. Lattice parameters of FeS at the lowest and highest pressure points shown for the troilite, MnP and FeS-III phases in Fig. 7.

$P$ (GPa)	$a$ (Å)	$b$ (Å)	$c$ (Å)	$\alpha$ (°)	$\beta$ (°)	$\gamma$ (°)
0	5.9655(3)	5.9655(3)	11.7512(3)	90	90	120
3.57	5.8648(5)	5.8648(5)	11.5960(4)	90	90	120
3.71	5.7393(2)	3.3765(1)	5.8073(2)	90	90	90
6.70	5.6565(3)	3.3331(2)	5.7288(3)	90	90	90
7.20	8.1354(3)	5.6863(2)	6.4996(3)	90	93.117(3)	90
10.15	8.0323(4)	5.6211(4)	6.4267(3)	90	92.862(5)	90

precision relative to the (small) pressure range in each phase to yield meaningful values of the ambient-pressure bulk modulus  $B_0$  and its pressure derivative  $B'$  in the MnP and FeS-III phases. However, the data in the troilite phase can be seen to lend some support to the negative  $B'$  reported for this phase by King and Prewitt.<sup>10</sup>

The transition from MnP to phase III is accompanied by (i) an abrupt volume decrease of 6.7(2)% (Ref. 20)—6.0(2)% in terms of  $\Delta V/V_0$  (Ref. 12)—that is mostly due to the contraction along  $C$  (Fig. 4); (ii) by metallization and the loss of magnetic order;<sup>2,10</sup> and (iii) by a marked decrease in Fe-Fe distances. The mean of Fe-Fe distances less than 3.0 Å falls more-or-less linearly through the troilite and MnP phases from 2.95 Å at ambient pressure to 2.85 Å just before the transition to phase III.<sup>8</sup> Immediately above that transition, it has decreased sharply to 2.70 Å. It had been thought previously that the contraction of the structure along  $C$  signaled an increased Fe-Fe interaction in that direction alone. Our results show that there is a similar strengthening in the basal planes. Goodenough concluded that the triangular clustering in the troilite phase [Fig. 6(a)] can be attributed to significant delocalization of the sixth, minority-spin  $3d$  electron, even at

ambient pressure.<sup>3</sup> The significant further shortening of the Fe-Fe distances accompanying the loss of the magnetic order suggests that the transition to phase III is driven by the Fe-Fe interactions and a distinct change in the  $3d$ -electron configuration.<sup>2</sup> The isomer shift and quadrupole splitting obtained from Mössbauer spectra in phase III (Refs. 2 and 10) led King *et al.*<sup>10</sup> to the unexpected conclusion that the iron in phase III may be Fe<sup>3+</sup>; and they rejected a high-spin to low-spin interpretation. However, the recent Mössbauer study by Kobayashi *et al.*<sup>2</sup> suggests that FeS may have a collapsed moment and be a Pauli paramagnetic metal in phase III. Clearly, a reanalysis of the Mössbauer data in the light of the full crystal structure would now be very interesting and informative.

In summary, the long-unknown structure of FeS-III has been solved. As for the lower pressure troilite and MnP phases, it is a distortion of the NiAs structure, characterized by clustering of the Fe atoms in the planes perpendicular to the equivalent of the NiAs unique axis. However, the Fe-Fe distances are markedly shorter, and the close coordination of one of the three independent Fe sites is distorted from FeS<sub>6</sub> to FeS<sub>5</sub>. These are the principal structural changes accompanying the loss of the magnetic order at the MnP to FeS-III transition.

We thank our colleagues J. S. Loveday, for much assistance with structural drawings, W. G. Marshall, for several helpful discussions, and M. R. Gibbs, D. R. Allan, and Y. Ko for assistance with some of the experimental work. We acknowledge technical support from G. Bushnell-Wye and A. A. Neild. This work was supported by a grant from the Engineering and Physical Sciences Research Council, funding from the Council for the Central Laboratory of the Research Councils, and by facilities made available by Daresbury Laboratory. M.I.M. acknowledges support from the Royal Society. J.B.P. acknowledges the support of the NSF through Grant No. EAR 95-06483.

\*Now at Department of Physics and Astronomy, The University of Edinburgh, Edinburgh, United Kingdom.

<sup>1</sup>O. Kruse, *J. Phys. Chem. Solids* **54**, 1593 (1993).

<sup>2</sup>H. Kobayashi, M. Sato, T. Kamimura, M. Sakai, H. Onodera, N. Kuroda, and Y. Yamaguchi, *J. Phys.: Condens. Matter* **9**, 515 (1997).

<sup>3</sup>J. B. Goodenough, *Mater. Res. Bull.* **13**, 1305 (1978).

<sup>4</sup>J.-P. Poirier, *Phys. Earth Planet. Inter.* **85**, 319 (1994).

<sup>5</sup>A. Weizman, D. Prialnik, and M. Podolak, *J. Geophys. Res.* **101**, 2235 (1996).

<sup>6</sup>E. Ohtani and N. Kamaya, *Geophys. Res. Lett.* **19**, 2239 (1992).

<sup>7</sup>L. A. Taylor and H. K. Mao, *Science* **170**, 850 (1970).

<sup>8</sup>H. E. King and C. T. Prewitt, *Acta Crystallogr., Sect. B: Struct. Crystallogr. Cryst. Chem.* **38**, 1877 (1982).

<sup>9</sup>H. K. Mao, G. Zou, and P. M. Bell, *Carnegie Inst. Wash. Publ.* **80**, 267 (1981).

<sup>10</sup>H. E. King, D. Virgo, and H. K. Mao, *Carnegie Inst. Wash. Publ.* **77**, 830 (1978).

<sup>11</sup>Y. Fei, C. T. Prewitt, H. K. Mao, and C. M. Bertka, *Science* **268**, 1892 (1995).

<sup>12</sup>K. Kusaba, Y. Syono, T. Kikegawa, and O. Shimomura, *J. Phys. Chem. Solids* **58**, 241 (1997).

<sup>13</sup>R. J. Nelmes, M. I. McMahon, S. A. Belmonte, D. R. Allan, M.

R. Gibbs, and J. B. Parise, *Rev. High Pressure Sci. Technol.* **7**, 202 (1998).

<sup>14</sup>R. J. Nelmes and M. I. McMahon, *J. Synchrotron Radiat.* **1**, 69 (1994).

<sup>15</sup>D. Louër and R. Vargas, *J. Appl. Crystallogr.* **15**, 542 (1982).

<sup>16</sup>The reflection indexed as (302) by Kusaba *et al.* (Ref. 12) is clearly indexed correctly as (013) in our patterns.

<sup>17</sup>Kusaba *et al.* (Ref. 12) propose that the monoclinic shear is in the basal plane, but that is inconsistent both with the space-group symmetry—for a NiAs-like structure—and also with a strong contraction along the NiAs  $C$  axis.

<sup>18</sup>The  $a$ -glide relates atoms  $a/2$  apart in the FeS-III structure, and this corresponds to atoms related by the  $a$ -glide operation plus a lattice repeat along  $b'$  in the MnP structure, i.e.,  $\mathbf{a}/2 = \mathbf{a}'/2 + \mathbf{b}'$ .

<sup>19</sup>R. B. Von Dreele and A. C. Larson (unpublished).

<sup>20</sup>Refinement of a mixed-phase pattern at 7.1 GPa gives  $a' = 5.6401(4)$  Å,  $b' = 3.3273(2)$  Å,  $c' = 5.7194(4)$  Å for the MnP phase, and  $a = 8.1350(5)$  Å,  $b = 5.6871(2)$  Å,  $c = 6.4994(5)$  Å,  $\beta = 93.11(4)^\circ$  for the FeS-III phase. The volume difference of 6.7(2)% is smaller than found in Ref. 8, but agrees with Ref. 12.

<sup>21</sup>N. G. Wright, R. J. Nelmes, S. A. Belmonte, and M. I. McMahon, *J. Synchrotron Radiat.* **3**, 112 (1996).